

CHEMISTRY

A European Journal

A Journal of



Accepted Article

Title: Photoinduced Thiol-ene chemistry applied to the synthesis of elastin-inspired self-assembling glycopeptides

Authors: Germano Piccirillo, Antonietta Pepe, Emiliano Bedini, and Brigida Bochicchio

This manuscript has been accepted after peer review and appears as an Accepted Article online prior to editing, proofing, and formal publication of the final Version of Record (VoR). This work is currently citable by using the Digital Object Identifier (DOI) given below. The VoR will be published online in Early View as soon as possible and may be different to this Accepted Article as a result of editing. Readers should obtain the VoR from the journal website shown below when it is published to ensure accuracy of information. The authors are responsible for the content of this Accepted Article.

To be cited as: *Chem. Eur. J.* 10.1002/chem.201604831

Link to VoR: <http://dx.doi.org/10.1002/chem.201604831>

Supported by
ACES

WILEY-VCH

Photoinduced Thiol-ene chemistry applied to the synthesis of self-assembling elastin-inspired glycopeptides

Germano Piccirillo,^{#[a]} Antonietta Pepe,^{#[a]} Emiliano Bedini,^[b] and Brigida Bochicchio^{*[a]}

Abstract: Synthetic (glyco-)peptides inspired by proteins able to self-assemble are appealing biomaterials in the field of tissue engineering and regenerative medicine. Herein for the first time, taking advantage of thiol-ene chemistry coupled to Solid Phase Peptide Synthesis, a self-assembling peptide inspired by elastin protein was bioconjugated to three carbohydrates in order to obtain the corresponding glycopeptides. They were studied at molecular and supramolecular level. The results show that the carbohydrate influences the molecular conformation of the glycopeptide and its self-aggregation properties as well. As future perspective, the results could enable us to tune the final self-aggregation properties of the glycopeptide by changing the sugar moiety.

Introduction

Elastin is the protein responsible for the elasticity of organs and tissues. It is a cross-linked polymer whose soluble precursor is tropoelastin exerting its elasticity in the Extracellular Matrix (ECM) together with other components, such as microfibril-associated glycoproteins (MAGPs), fibulins, and fibrillins. All of them are present in the form of fibers considered crucial for the exerted biological role^[1]. Elastin is widely considered as an inspiring protein for the design of biomaterials due to its poor immunogenicity and high biocompatibility^[2]. Furthermore, elastin is characterized by repetitive motifs thoroughly repeated along the primary structure and considered significant for its function. Short elastin-inspired peptides constituted of these repetitive motifs are an interesting class of self-assembling materials able to give rise to fibrils despite of their small size^[3]. In that context, glycine-rich sequences where the XGGZG motif (X, Z = V, L) is three-fold repeated were demonstrated to be prone to self-aggregation^[4]. Among them, (LGGVG)₃ self-aggregated into intertwined fibers with a regular pitch of the helix^[3a]. That finding lets us consider it as a model peptide for useful applications in the nanotechnology field.

Glycosylated peptides are gaining increasing interest in tissue

engineering and regenerative medicine for their ability in directing cells to normal development and tissue repair^[5]. Besides, some peptide-carbohydrate conjugates able to self-assemble and to form nanoaggregates in the form of fibers, micelles and spherical particles represent an added value for various applications, such as bacterial agglutination, drug-delivery, and vaccines^[6]. While the synthesis of standard peptides has become routine and can be readily accomplished via automated methods, the synthesis of glycopeptides can be significantly more challenging^[7]. Generally, the preparation of glycopeptides has been realized by attaching carbohydrates to side-chains of amino acid residues such as lysine, cysteine, serine and threonine. Conjugation in solution can be performed by chemoselective ligation techniques involving the formation of disulfide, thioether, thioester, oxime, hydrazone linkages^[8]. However, some ligation techniques - e.g. oxime bond forming ones - can suffer from low yields, lower purity, dimerization byproducts, and acid lability, among other drawbacks^[9]. Click chemistry has gained high attention for the synthesis of biomaterials thanks to the efficiency of click couplings in mild conditions and at low concentrations. Sharpless introduced the concept of click chemistry referred to reactions carried out on aerobic and atmospheric pressure conditions^[10]. Thiol-ene click chemistry (TEC) represents an emergent ligation strategy^[11] based on the photo-induced coupling of an olefin with a sulfhydryl group in mild conditions^[12]. TEC methodology is essentially based on the alkene hydrothiolation reaction that occurs by a radical mechanism with anti-Markovnikov regioselective orientation^[13]. Some attempts were made to investigate TEC methodology in order to prepare glycosylated amino acids, peptides and proteins in solution^[12, 14]. Here, we describe the synthesis of three glycosylated amino acids obtained by coupling different O-allyl carbohydrates with *N*-9-Fluorenyl-methoxy-carbonyl-L-cysteine (Fmoc-L-cysteine) via TEC. These derivatives were then conjugated via Solid Phase Peptide Synthesis (SPPS) to a self-assembling elastin-derived peptide. SPPS represents a versatile and clean synthetic methodology that also allowed us to avoid the early undesired aggregation of the peptidic moiety. Concerning carbohydrates, our attention was focused on three α -glycosides (L-rhamnopyranoside, D-galactopyranoside, and D-mannopyranoside) because of their appealing biological properties^[15]. For example, L-rhamnose has been recently evidenced to be involved in recognition events by human immune system^[16] as already known for mannose and galactose oligosaccharides. Furthermore, galactose has been widely employed in tissue engineering application, because it supports hepatocyte adhesion and enhances cell functions as a consequence of the interactions with asialoglycoprotein

[a] ^{#[a]}Mr. G. Piccirillo, ^{#[a]}Prof. A. Pepe, Prof. B. Bochicchio
Department of Science
University of Basilicata
Via Ateneo Lucano, 10
85100 Potenza, Italy. ^{#[a]}The authors equally contributed to the work
E-mail: brigida.bochicchio@unibas.it

[b] Dr. E. Bedini
Department of Chemical Sciences
University of Naples Federico II
Complesso Universitario Monte S. Angelo,
Via Cintia, 4
80126 Naples, Italy

Supporting information for this article is given via a link at the end of the document.

Table 1. Chemical structure of the synthesized glycopeptides **9a-c**

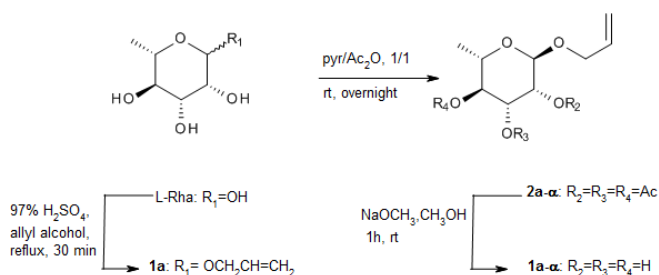
Carbohydrate derivative ^[a]	Chemical Structure	MW (Da)
α -L-rhamnopyranosyl		1531.77
α -D-galactopyranosyl		1547.77
α -D-mannopyranosyl		1547.77

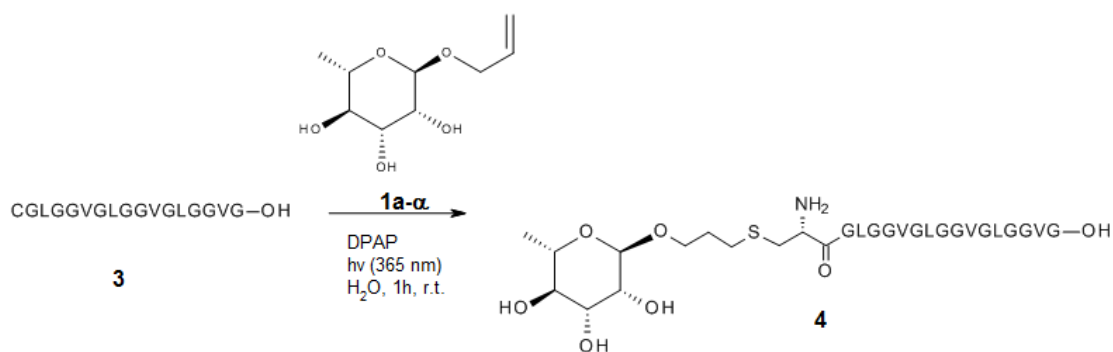
receptors.^[17] The three synthesized bioconjugates are shown in Table 1. All of them share the amino acid sequence GLGGVGLGGVGLGGVG inspired by the elastin-derived peptide (LGGVG)₃^[3a]. However, the original sequence has been modified through the addition at N-terminus of a glycine as a spacer. Circular dichroism (CD), nuclear magnetic resonance (NMR) and Fourier transform-infrared (FT-IR) spectroscopies were used in order to assess the effects of carbohydrate modifications on the molecular conformation of the glycopeptides. The self-assembling properties were assessed by turbidimetry and the aggregates characterized by transmission electron (TEM), scanning electron (SEM) and atomic force (AFM) microscopies.

Results and Discussion

Synthesis of the allyl glycoside of L-rhamnose. The synthesis of the allyl glycoside of L-rhamnose **1a** (Scheme 1) was conducted by treating it in refluxing allyl alcohol with concentrated sulfuric acid, as already reported^[18]. An α/β anomeric mixture with a marked predominance of the thermodynamically preferred α -glycoside (12:1) was obtained in

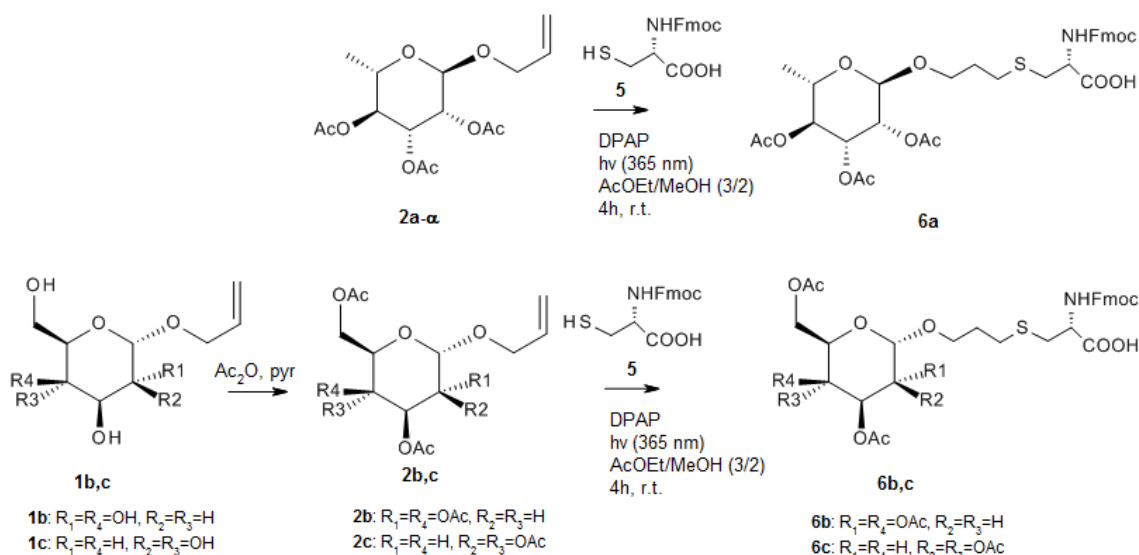
72% yield. Since chromatographic attempts to separate the two anomers by silica gel chromatography failed, a per-*O*-acetylation of the mixture was performed, followed by purification of the 2,3,4-tri-*O*-acetylated allyl α -glycoside **2a- α** (86%, Scheme 1). Cleavage of acetyl groups by Zémlen transesterification then gave allyl- α -L-rhamnopyranoside **1a- α** (96%) in pure form.

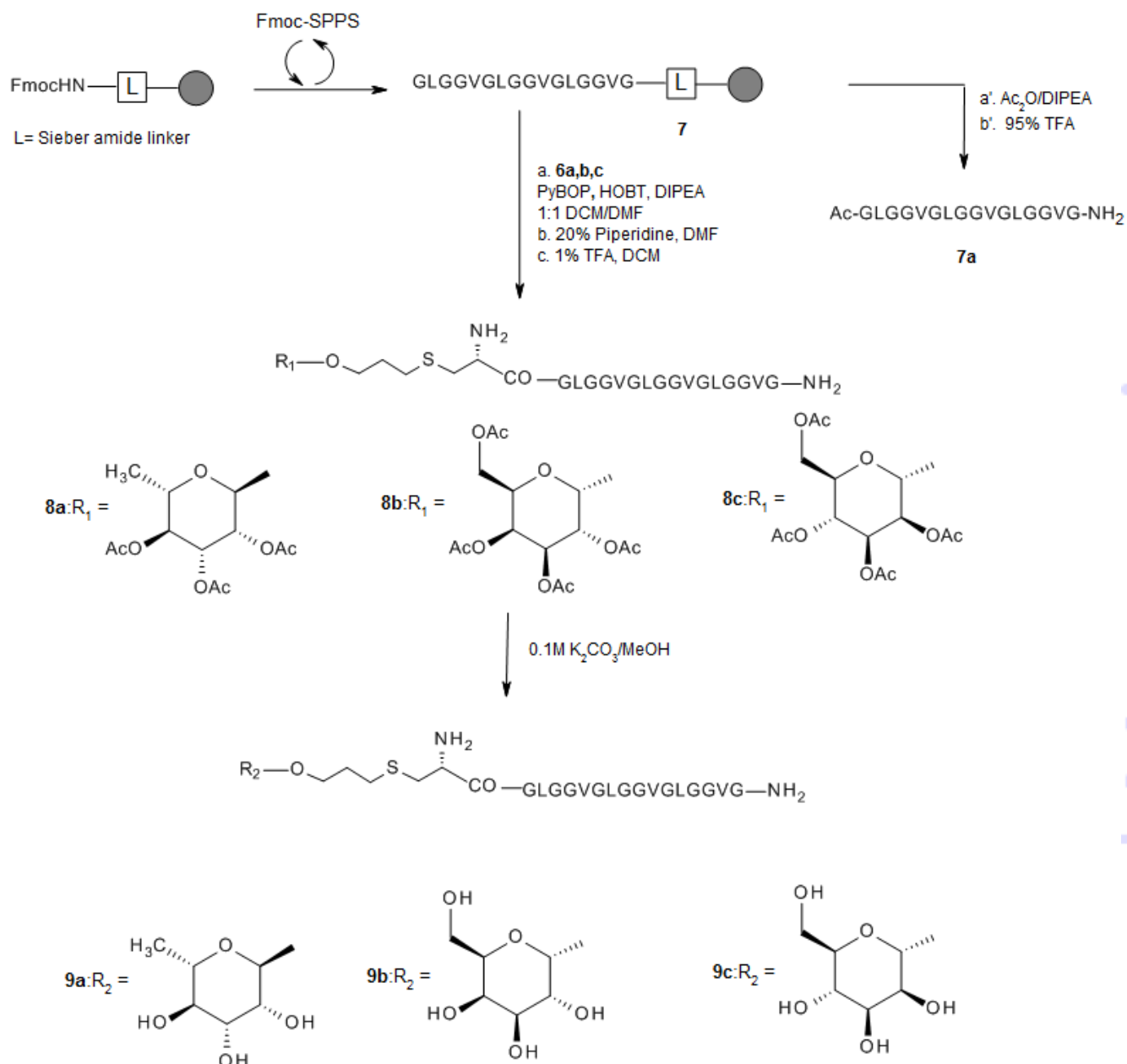
**Scheme 1.** Synthesis of allyl rhamnoside **1a- α** .

Scheme 2. Synthesis of glycopeptide **4**.

Synthesis of elastin-inspired glycopeptides. The first attempt to synthesize an elastin-inspired glycopeptide by thiol-ene reaction was performed in solution by reacting peptide **3** with the allyl rhamnoside **1a- α** (Scheme 2). Peptide **3**, synthesized by solid-phase peptide synthesis (SPPS), was photochemically coupled through the side-chain free thiol group of cysteine to allyl α -L-rhamnopyranoside **1a- α** by adding catalytic amounts of 2,2-dimethoxy-2-phenylacetophenone (DPAP) as initiator in methanol/water (1:2, v/v). The desired glycopeptide **4** was obtained after purification in low amount (26%). Therefore, we explored as alternative strategy the synthesis of the glyco-conjugated cysteine intermediates **6a,b,c** (Scheme 3) eligible to be coupled by SPPS to peptide-resin **7** in order to obtain glycopeptides **9a,b,c** (Scheme 4). The idea was

to take advantage of SPPS in order to easily manage a product prone to self-aggregation. Furthermore, the acetylation of hydroxyl groups of allyl carbohydrates **1b,c** (Scheme 3) was carried out in order to avoid undesired side-chain reactions. The incorporation of cysteine derivatives during SPPS is well-known for its high propensity to racemization under standard coupling conditions^[19]. In order to limit epimerization the coupling of the glyco-conjugated cysteine intermediates **6a,b,c** was conducted manually in conditions that ensure a safe incorporation with minimal racemization (Scheme 4). In particular, the pre-activation step was avoided, the amount of base was reduced and a less polar solvent mixture (DMF/DCM; 1/1, v/v) was employed^[19].

Scheme 3. Synthesis of the glyco-conjugated cysteine intermediates **6a,b,c**.



Scheme 4. Synthesis of the glycopeptides **9a,b,c**.

Finally, acetyl groups in glycopeptides **8a,b,c** were removed in order to obtain glycopeptides **9a,b,c** (Scheme 4) in a 3:2 ratio with the non-conjugated GLGGVGLGGVGLGGVG-NH₂ peptide. The final products **9a,b,c** were recovered after purification by RP-HPLC in yields of 56, 58 and 55%, respectively.

Spectroscopy studies. FT-IR studies provided insightful information concerning the effects of modification on the secondary structure of the peptide triggered by the

bioconjugation of the peptide with the carbohydrate both in the pre-aggregated and in the post-aggregated state (Table 2, Figures S23-S32 in Supporting Information). Additionally, in order to have useful insights on the conformation of the pre-aggregated state, CD analysis was carried out in aqueous and fluorinated solvents and as a function of the temperature as well. The CD spectrum of glycopeptides **9a** is shown in Figure 1a. In aqueous solution the CD spectrum at 273 K shows a strong negative band centred at 195 nm and a small positive one at

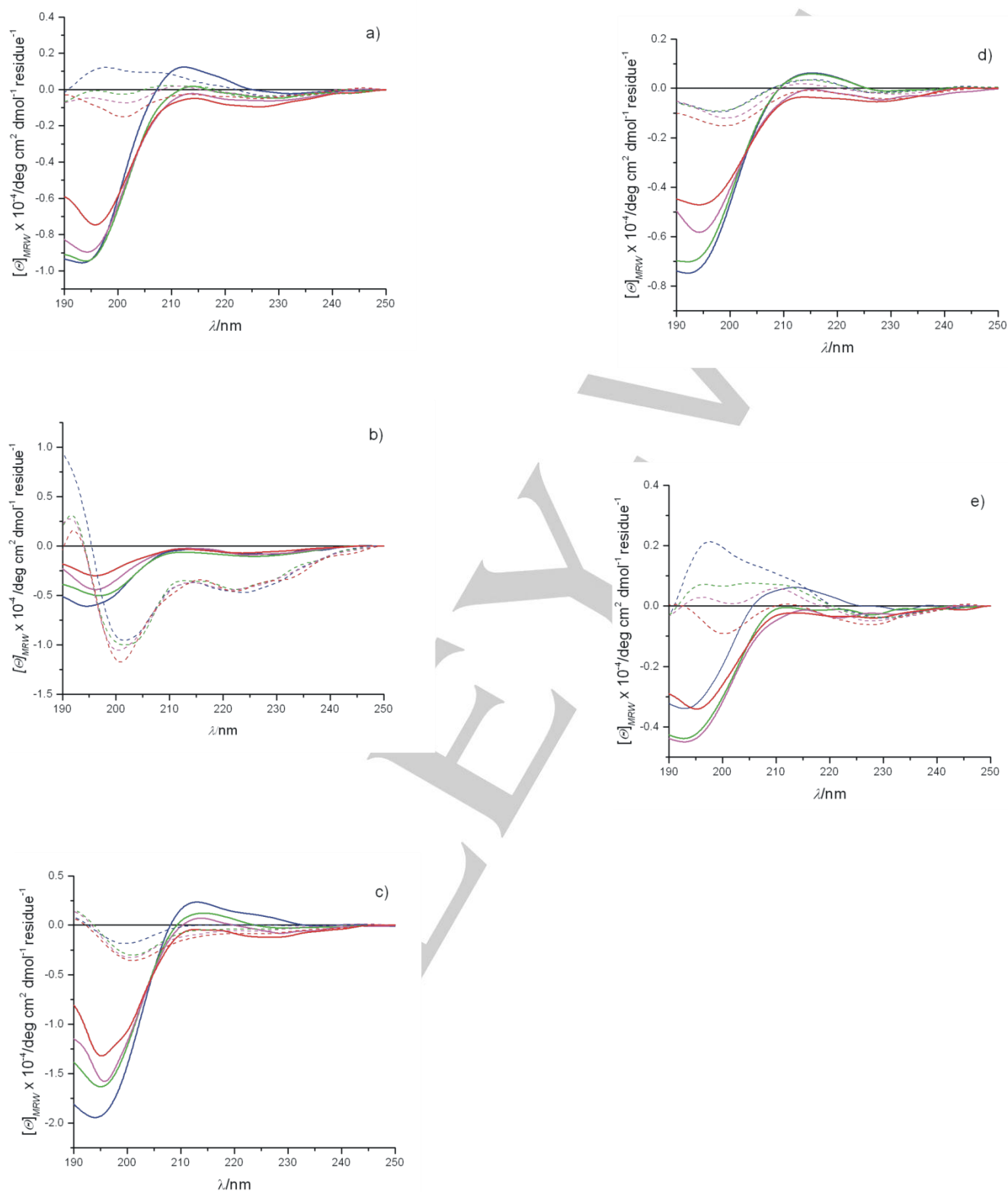


Figure 1. Temperature-dependent CD spectra. CD spectra recorded at 273 K (blue), 29°C (green), 310 K (magenta) and 333 K (red) in aqueous (solid line) and TFE solution (dashed line) of (a) glycopeptide 9a, (b) glycopeptide 9b, (c) glycopeptide 9c, (d) peptide 3 and (e) peptide 7a.

Table 2. Assignments and relative areas of amide I components of FT-IR spectra in the pre-aggregated and post-aggregated state.

	3		7a		9a		9b		9c		Assignments
	ν (cm^{-1})	A (%)									
Pre-aggregation ^[a]	1631	11.9					1635	29.3			β -sheet random coil PPII β -turn antip. β -sheet
	1650	22.6	1642	40.8	1646	29.8	1652	33.9	1645	47.9	
	1668	25.4	1671	40.8	1667	30.3	1674	28.2			
	1681	23.1			1681	26.4			1679	52.1	
	1699	17.0	1697	18.4	1701	13.5	1696	8.7			
Post-aggregation ^[b]	1631	51.7	1630	41.5	1614	19.3	1630	44.3	1630	29.6	Cross- β β -sheet β -sheet random coil loops PPII β -turn antip. β -sheet
	1652	26.7			1630	41.5			1637	29.9	
			1660	29.7	1650	19.5					
	1675	16.4			1671	12.5	1662	31.5	1661	17.4	
	1696	5.1	1695	28.7	1695	8.2	1698	24.2	1679	13.6	
								1698	9.5		

[a] samples were analyzed after freeze-drying. [b] samples were analyzed after turbidimetry studies; the components between 1610-1600 cm^{-1} , arising from side-chain vibrations, are not included in the calculations, as well as the component at 1740-1745 cm^{-1} , arising from C-terminal COOH.

212 nm. The negative maximum near 197 nm is characteristic of the CD spectra of unordered peptides, but the poly-L-proline II (PPII) conformation also gives such band^[20]. The presence of PPII is also suggested by the positive band at 212 nm that is a distinctive feature of the CD spectra of PPII conformation^[20a]. However, the value for $[\theta]_{195}$ ($-10,000 \text{ deg cm}^2 \text{ dmol}^{-1}$) is compatible only with a small fraction of PPII^[21]. The increase of the temperature to 298, 310 and 333 K induces the loss of the positive band and the gradual decrease of the negative one together with a slight red-shift suggesting the progressive destabilization of PPII conformation as a function of the temperature and the increase of the contribution from β -turn and β -sheet. The CD spectrum at 273 K in TFE shows two small positive bands centred at 197 and 209 nm that suggest the tendency by the glycol-conjugate to adopt a type II β -turn^[22]. The positive bands disappear at 298 and 310 K while at 333 K a small negative band, centred at 202 nm, appears thus suggesting the destabilization of the turn. The FT-IR data confirm the presence of multiple conformations (Table 2).

The CD spectrum of glycopeptide **9b** is shown in Fig. 1b. In aqueous solution the CD spectrum at 273 K is characterized by a weak negative band at 194 nm decreasing on increasing the temperature. The small intensity of the negative band, compared to a CD negative band expected for a fully unordered peptide, suggests the co-presence of β -turn and β -sheet in equilibrium with random coil conformation. FT-IR data confirm this finding, showing that glycopeptide **9b** is the only compound with a discrete percentage of β -sheet before aggregating (Table 2). Actually, β -turn and β -sheet conformations are characterized by

CD spectra with positive bands in the range 195-210 nm that could be responsible for the low intensity of the observed negative band occurring in the same wavelength range. In TFE, the CD spectra dramatically change. At 273 K it shows a strong positive band at 190 nm and two smaller negative bands at 201 and 222 nm indicating the presence of a type I β -turn. At higher temperatures, the strong positive band strongly decreases while the negative band at 201 nm slightly increases suggesting the destabilization of β -turn conformation. Conformational analysis by NMR of the glycopeptide **9b**, recorded in TFE- d_3 H₂O (80/20, v/v), confirmed the presence of a turn structure spanning GVGL amino acidic residues. Discernible NMR features of the β -turn are $d_{\alpha N}(i,i+2)$ and $d_{NM}(i,i+2)$ medium range NOEs involving V and L residues. Given the presence of the three-fold repeated LGGVG motif along the sequence and the close similarity of the chemical shifts of amide and H α protons of the residues belonging to repeated sequences, the exact localization of the turn at G⁵VGL⁸ or G¹⁰VGL¹³ is not possible. Consequently, a precise molecular model of the glycopeptide **9b** in fluorinated solvent is not achievable. Interestingly, the GVGL turn was not previously detected in the pristine peptide devoid of the carbohydrate^[3a]. Therefore, it has been demonstrated that the bioconjugation with the galactoside moiety induces the adoption of specific conformations for the peptide chain.

The CD spectrum of glycopeptide **9c** is shown in Fig. 1c. The CD spectrum at 273 K shows a strong negative band at 194 nm and a small positive one at 214 nm. Both bands decrease on increasing the temperature. These spectral findings are indicative of the presence of a small amount of PPII

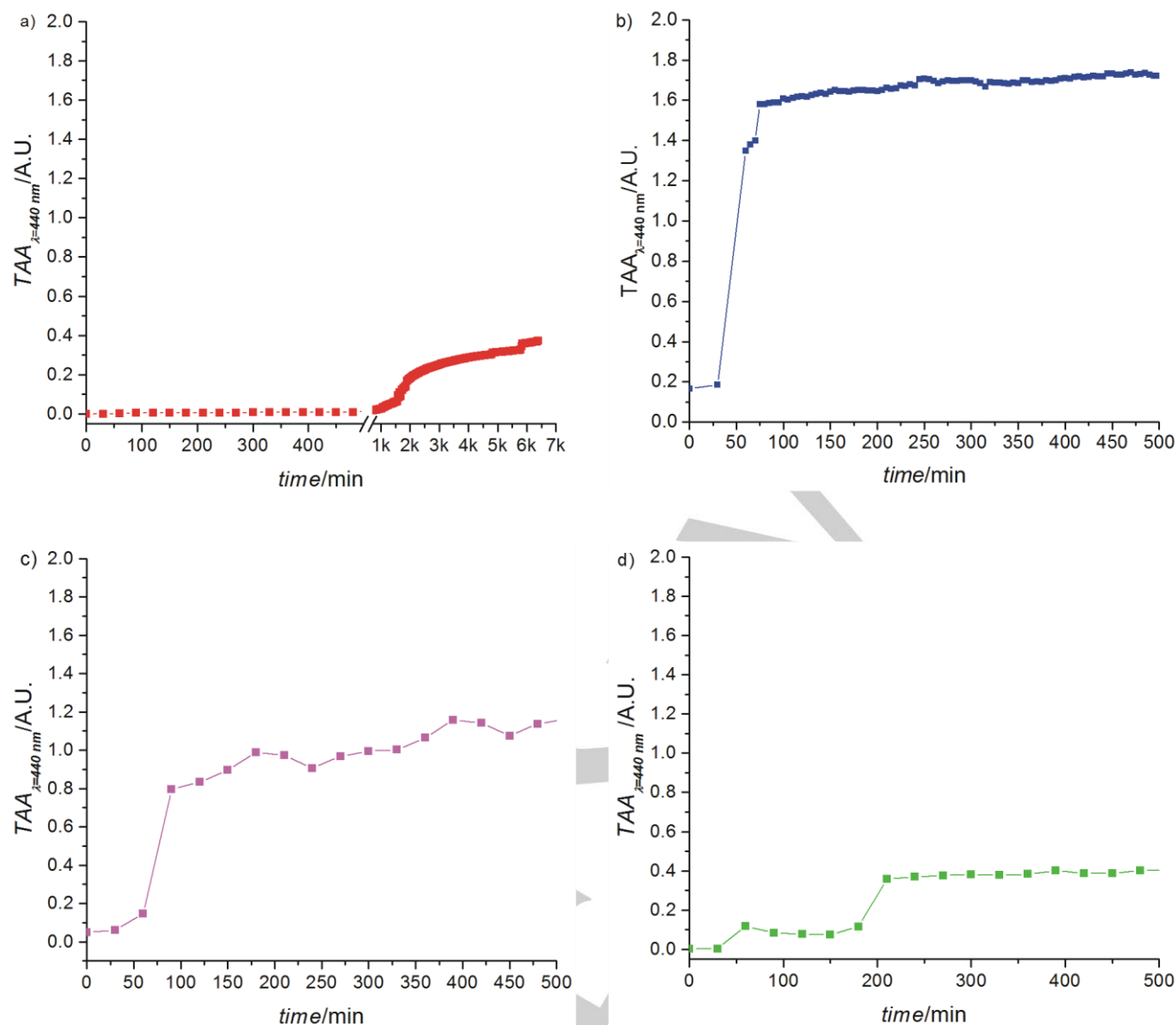


Figure 2. Turbidimetric determination of the self-assembly of a) glycopeptide **9a**; b) glycopeptide **9c**; c) peptide **3**; d) peptide **7a**

conformation, together with random coil, proved by the persistence of the positive band even at 333 K. In TFE, the CD spectrum at 273 K shows a small negative band at 201 nm decreasing with increasing temperature. Such spectral features are indicative of the presence of turn structures together with extended conformations, such as PPII, and random coil. According to CD analysis, the decomposition of the FT-IR spectrum of the pre-aggregated state of glycopeptide **9c** shows an high percentage area assigned to β -turn and random coil conformations (Table 2).

The CD spectrum of peptide **3** is shown in Fig. 1d. In aqueous solution the CD spectra at 273 and 298 K are characterized by a negative band at 191 nm and a small positive band at 215 nm suggesting the presence of PPII conformation with a certain percentage of random coil and β -turns. The increase of the temperature to 310 and 333 K triggers the decrease of both

bands suggesting the destabilization of PPII and the stabilization of β -turns. In TFE, the CD spectrum at 273 K shows a small negative band at 199 nm gradually decreasing at higher temperatures. These spectral findings are assigned to presence of turns together with random coil conformations. FT-IR analysis shows for peptide **3** in the pre-aggregated state a discrete percentage of β -sheet, as expected for FTIR in solid state, with the co-presence of random coil, PPII and β -turn conformations. The CD spectrum of peptide **7a**, lacking cysteine residue, is shown in Figure 1e. In aqueous solution the CD spectrum at 273 K is characterized by a weak negative band at 192 nm and a small positive band at 214 nm. The CD spectra at 298 and show the increase of the negative band and the loss of the positive one. At 333 K the negative band further decreases. These spectra suggest the presence of PPII conformation,

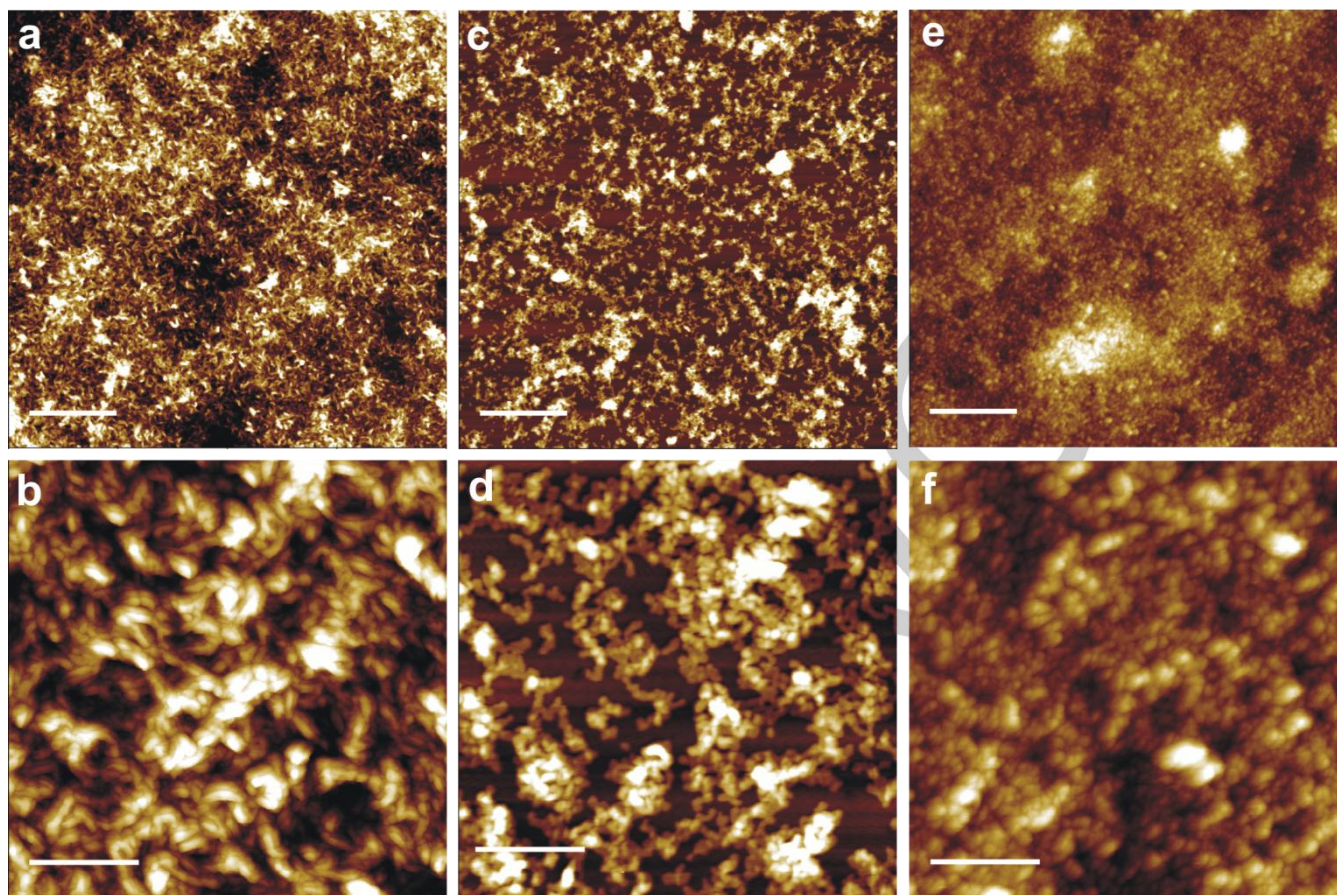


Figure 3. AFM images of the aggregates formed after turbidimetry assay by glycopeptide **9a** (a, b); glycopeptide **9b** (c, d); glycopeptide **9c** (e, f). The bars in panel a, c, e represent 2 μm while in panel b, d, f 0.5 μm .

stable at 273 K, together with unordered conformations prevalent at high temperatures. In TFE, the CD spectrum at 273 K shows a weak positive band at 198 nm even decreasing with the temperature and a weak shoulder at 210 nm. The CD features are indicative of the presence of small amounts of β -turn and β -sheet together with unordered conformations. Finally, the CD spectrum at 333 K shows a small negative band at 200 nm and a tendency toward a positive one at 212 nm, probably due to a small contribution of PPII conformation. FT-IR data confirm the presence of PPII helix in the pre-aggregated state while β -sheets prevail in the post-aggregated one.

FT-IR in the solid state of the post-aggregated phase (Table 2), shows for all compounds huge amounts of β -sheet conformation, as expected for the strongly hydrogen bonded aggregated samples. Interestingly, glycopeptide **9a** shows some percentage of cross- β conformation.

Supramolecular studies

Self-assembling peptides are able to form assorted supramolecular structures ranging from nanofibers, sheets and tapes to spheres and networks. The morphology of the aggregates is strongly influenced by the sequence of the peptide and the environmental conditions. Furthermore, many self-assembling peptides respond to external environmental stimuli

able to trigger the aggregation, like pH, temperature, and solvent^[23]. Additionally, the presence of conjugated molecules may exert an important influence on the aggregation process. For example, hydrophobic tails present in the amphiphilic peptides or aromatic groups, such as 9-fluorenylmethoxy moiety, in Fmoc-peptides drive the assembly in fibrous hydrogels by hydrophobic and π - π interactions, respectively^[24].

In order to define the role of the specific glycans in the self-assembly of glycoconjugates, we performed the aggregation studies of the glycopeptides by turbidimetry assay and compared the results with the non-decorated peptides **3** and **7a**. Turbidimetric measurements can be used to monitor aggregation in a simple way, giving us qualitative information on how the aggregation process evolves with time. The intensity of turbidimetry on apparent absorbance (TAA) depends mainly on the size and the number of aggregates in suspension. As shown in Figure 2, all the peptides show a typical sigmoidal curve.

A remarkable difference among the graphs is observed in the lag phase and in the TAA values reached at the plateau. The glycopeptide most prone to aggregation is glycopeptide **9b**, aggregating in few minutes (data not shown), followed by glycopeptide **9c** and peptide **3**, showing the highest TAA values, 1.7 and 1.2, respectively. The model peptide **7a** requires more than 3 hrs to aggregate (Figure 2d), while glycopeptide **9a**

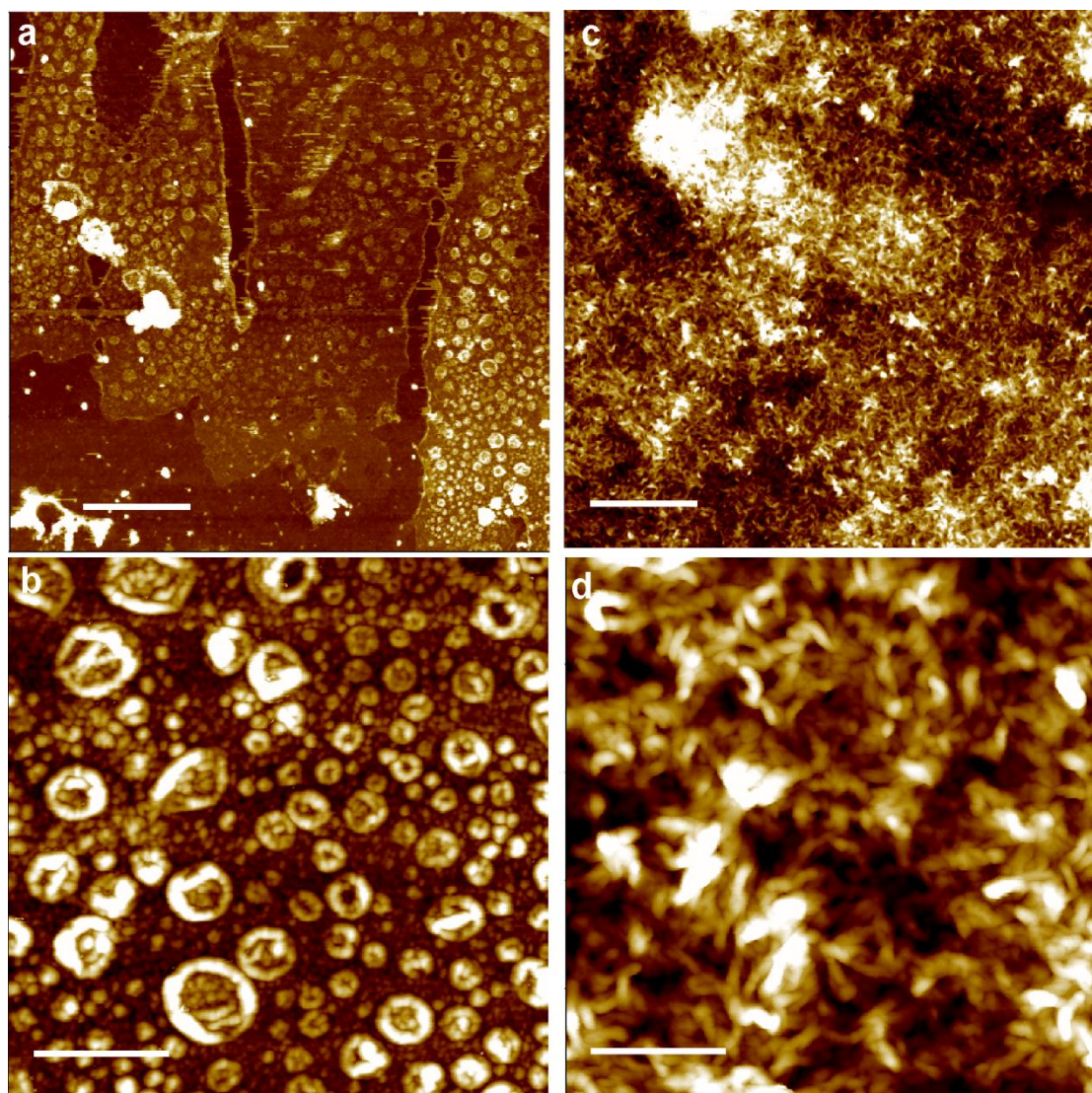


Figure 4: AFM images of the aggregates formed after turbidimetry assay by peptide **3** (a, b) and peptide **7a** (c, d). The scale bars in panel a and c indicate 2 μm ; in panel b and d the scale bars indicate 0.5 μm .

requires more than 24 hrs, with a final TAA value of 0.32 (Figure 2a). Thus we conclude that the glycopeptide **9a** is the one with lower tendency to aggregate under the used experimental conditions. Taken together, our data show that TAA values at the plateau are inversely correlated with the aggregation lag phase.

In order to have a deeper insight into the supramolecular structures of the aggregates, we performed studies by AFM, TEM and SEM microscopies as well.

AFM is widely used in order to analyse the morphology of nanostructures formed by self-assembling molecules^[25]. Small aliquots of the samples after aggregation were deposited on silicon wafers and after air-drying analysed by AFM. In Figure 3 the formed aggregates after turbidimetry analysis by

glycopeptides **9a**, **9b**, and **9c** are shown. AFM data show that the morphology is significantly dependent on the nature of the carbohydrate. Glycopeptide **9a** shows the formation of entangled flake-like structures (Figure 3a,b), while glycopeptide **9b** shows the formation of fibrils prone to evolve in fibers (Figure 3c,d). Glycopeptide **9c** presents a carpet of globular structures (Figure 3 e,f).

The nanostructures formed by the model peptide **3** and **7a**, without the carbohydrate group, are shown in Figure 4.

Peptide **7a** evidences a morphology very similar to those observed for glycopeptide **9a**, with entangled flake-like structures (Figure 4c, d), while peptide **3**, containing an *N*-terminal cysteine shows highly peculiar structures (Figure 4a, b).

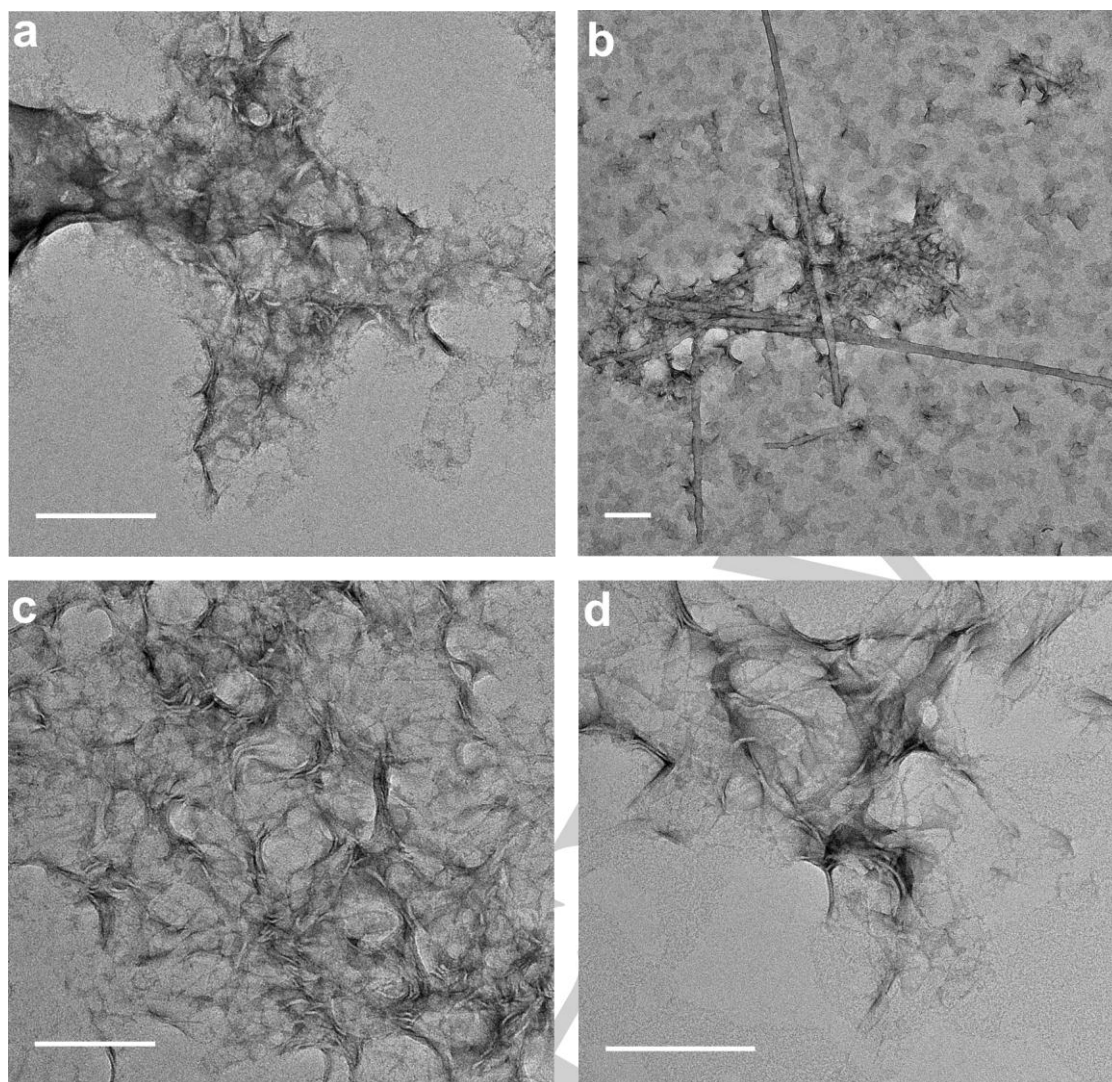


Figure 5: TEM images of a) glycopeptide **9a**; b) glycopeptide **9b**; c) peptide **3**; and d) peptide **7a**. Scale bars indicate 200 nm.

The film visible in Figure 4a contains basket-like structures, particularly evident at higher magnification (Figure 4b). The observed structures point to the formation of hollow nanospheres, that with air-drying could give rise to open vesicles. The same samples were studied also by TEM in order to have deeper insights into the fine supramolecular structure.

All the peptides display considerable self-aggregation forming nanostructures, whose morphological features are characterized by a mixture of fibrils and large clumps of protofibrillar aggregates, particularly evident for glycopeptide **9a** (Figure 5a) and for peptide **7a** (Figure 5d). Consistent with the reduced lag phase observed in turbidimetry experiments implying a higher aggregation propensity, glycopeptide **9b** shows the presence of straight ribbons (Figure 5b), that at higher magnification, result from lateral association of fibres (Figure S33 in Supporting Information). In the background, evolving protofibrils, previously observed in AFM images, are also discernible. By contrast, TEM

images for mannose-peptide **9c** lack evidence of higher-order assembled structures. The TEM grid was mostly blank with the occasional formation of amorphous aggregates (data not shown). By comparing AFM and TEM images of the nanostructures of the glycopeptides **9a**, **9b**, **9c** and peptide **3** and **7a**, we observe striking differences in the morphology of the nanostructures mainly for peptide **3**. While in AFM a film with vesicle-like structures is observed (Figure 4a and b), in TEM a wrapped film, with some protofibrils, is evident (Figure 5c). The high dehydration encountered during the observation by TEM microscopy has likely altered the morphology of the weak vesicular nanostructures formed by peptide **3**. The aggregates were analysed also by SEM, where the nanostructures were coated with a subtle film of gold prior to dehydration and observation, and globular structures are confirmed (Figure S34 in Supporting Information).

Summarizing, clear differences at molecular level detected by CD spectroscopy are evident for the three glyco-conjugates (Figure 1). A dominant type I β -turn is adopted only by glycopeptide **9b** while glycopeptides **9a** and **9c** take a mixture of random coil, β -turn and PPII conformations. At supramolecular level, slight variations are evident for the glycopeptide aggregates (Figures 3 and 5). With carbohydrate introduction, additional hydrogen bonding interactions involving hydroxyl groups of sugar moieties and peptide amide groups occur. These modifications also affects the supramolecular interactions in the aggregated state. According to our results, the pattern of hydrogen bonding is dependent on the stereochemistry of the carbohydrate. Galacto- and manno-pyranose are diastereoisomers belonging to aldohexose series and differ for their configurations at C-2 and C-4. The peculiar orientation in the space could be responsible for the observed differences. Moreover, for a deoxyhexose such as rhamnopyranose an additional variable to be taken into account is the smaller number of hydroxyl groups limiting the number of hydrogen bonds.

Conclusions

Herein, the chemical synthesis of three glyco-conjugated elastin-inspired peptides was accomplished through thiol-ene photo-induced coupling between per-*O*-acetylated allyl glycosides and Fmoc-cysteine, followed by SPPS. It has been demonstrated, by spectroscopy and microscopy studies, that the insertion of the carbohydrate has a significant effect on the specific conformation adopted and consequently on the self-assembly propensity of the bioconjugated molecules. The differences could be ascribed to the different chemical structure and stereochemistry of each carbohydrate. As future perspective, deeper insights into the self-aggregation mechanism could be given by further studies involving computational methodologies for Molecular Modeling and Dynamics. Moreover, we would like to demonstrate that the functionality of the sugar moiety is maintained in the here described glyco-conjugates^[26] in order to be recognized by specific cellular receptors^[17b, 27].

Experimental Section

Materials. All solvents and reagents were used as supplied. HPLC grade ACN, DMF were purchased from Romil Ltd. (Cambridge, UK). Diisopropylethylamine (DIEA), 1-hydroxybenzotriazol hydrate (HOBT-H₂O), DCM, piperidine, pyridine (pyr), acetic anhydride (Ac₂O), trifluoroacetic acid (TFA), dimethylaminopyridine (DMAP), 2,2-dimethoxy-2-phenylacetophenone (DPAP), triisopropylsilane (TIS), allyl α -D-galactopyranoside and allyl α -D-mannopyranoside were purchased from Sigma-Aldrich (Germany). 2-[[1H-benzotriazol-1-yl]-1,1,3,3-tetramethyluronium hexafluorophosphate (HBTU), (benzotriazol-1-yloxy)tripyrrolidinophosphonium hexafluorophosphate (PyBOP), Wang resin and Sieber Amide resin were purchased from Novabiochem (Darmstadt, Germany). Fmoc-amino acids were obtained from Inbios (Pozzuoli, Naples, Italy). Tris(2-Carboxyethyl)-Phosphine hydrochloride (TCEP) was purchased from Pierce.

General Experimental Methods. Nuclear magnetic resonance (NMR) spectra were acquired at room temperature on a Varian Inova 500 spectrometer operating at 500 MHz for ¹H nuclei and 125 MHz for ¹³C nuclei or on a Bruker DRX-400 (¹H: 400 MHz, ¹³C: 100 MHz). Reference peaks for ¹H and ¹³C spectra were respectively set to δ 7.26 ppm and δ 77.0 ppm for CDCl₃, δ 2.49 ppm and δ 39.5 ppm for DMSO-*d*₆, and δ 4.79 ppm for ¹H spectra in D₂O. NMR data were reported in values of chemical shift as parts per million (ppm) on the δ scale, and coupling constants in hertz (Hz). The conformational analysis by ¹H-NMR spectroscopy of galacto-peptide **9b** in TFE-*d*₃/H₂O (80/20, v/v) is described in Supporting Information (SI). Before characterization the (glyco-)peptides were purified by semi-preparative reversed phase high-performance liquid chromatography on a Shimadzu automated HPLC system supplied with a semipreparative Jupiter C18 column (Phenomenex, 250 x10 mm, 5 micron). The eluents were A (0.1% TFA in H₂O) and B (0.1% TFA in CH₃CN). A binary gradient from 5 to 60% B was used. ESI Mass spectrometry analysis was performed on the mass spectrometer Quattro Micro (Waters), equipped with a triple quadrupole and an electrospray source. MALDI-TOF spectrometry analysis was performed by CEINGE (Naples, Italy). Thin layer chromatography (TLC) was performed on Merck Kieselgel F254 200 μ m silica plates. Ultraviolet light at 254 nm was used as a visualizing agent. Alternatively, the plates were developed with 5% H₂SO₄ ethanolic solution and then heating to 230 ° C. Merck Silica gel60 (0.063-0.200 mm) was used for column chromatography. All UV reactions were carried out in a Photochemical Multirays Reactor (Helios-Italquartz, Milan, Italy) equipped with ten 15 W lamp whose output was centered at 366 nm.

Allyl α -L-rhamnopyranoside (**1a- α**):

A suspension of L-rhamnose monohydrate (1.035 g, 5.683 mmol) in allyl alcohol (13 mL) was refluxed at 100°C. After 10 min stirring a clear solution was obtained. It was cooled to room temperature, then treated quickly with 97% sulfuric acid (100 μ L) and heated again to 100°C. After 30 min stirring at this temperature, TLC analysis (5:2 v/v ethyl acetate-ethanol) showed complete consumption of the starting compound. The reaction was worked-up by cooling to room temperature and then neutralizing by addition of anhydrous potassium carbonate. The mixture was filtrated and concentrated to give a residue, that, after a column chromatography (18:1 to 10:1 v/v chloroform-methanol), afforded a 12:1 α/β anomeric mixture of allyl L-rhamnopyranoside **1a** (830 mg, 72%) as a colourless oil. This mixture (819 mg, 4.017 mmol) was dissolved in 1:1 v/v pyridine/acetic anhydride (8 mL) and the solution was stirred at rt overnight. TLC analysis (5:2 v/v toluene-ethyl acetate) showed complete consumption of the starting compound. The solution was diluted with CH₂Cl₂ (100 mL) and washed with 0.5 M HCl (100 mL). The organic phase was collected, dried over anhydrous Na₂SO₄, filtered and concentrated. The obtained residue was subjected to a column chromatography (6:1 to 4:1 v/v toluene-ethyl acetate) to give pure allyl 2,3,4-tri-*O*-acetyl- α -L-rhamnopyranoside (**2a- α** , 1.135 g, 86%) as a colourless oil. ¹H-NMR spectroscopic analysis of **2a- α** returned signals in full agreement with literature reference^[28].

Compound **2a- α** (926.6 mg, 2.808 mmol) was dissolved in methanol (12 mL) and treated with a 1.77 M methanolic solution of sodium methoxide (950 μ L, 1.682 mmol). After 60 min stirring at rt, TLC analysis (5:2 v/v ethyl acetate-ethanol) showed complete consumption of the starting compound. The reaction mixture was neutralized with Amberlyst® 15 (H+ form), filtered and concentrated. The obtained residue was subjected to column chromatography (15:1 to 12:1 v/v chloroform-methanol) to give pure **1a- α** (548 mg, 96%) as a colourless oil. ¹H-NMR spectroscopic analysis of **1a- α** returned signals in full agreement with literature reference^[29].

Peptide CGLGGVGLGGVGLGGVG-OH (3): SPPS synthesis was accomplished as described in Supporting Information.

α -L-Rhamnopyranosyl-conjugated peptide (4): Peptide **3** (30 mg, 22.6 μ mol) and allyl α -L-rhamnopyranoside **1a- α** (5 mg, 24 μ mol) were dissolved in MilliQ water (30 mL). Then DPAP (0.8 mg, 3 mmol) was added. The reaction mixture was poured in quartz tubes and irradiated for 1 h under stirring at 366 nm in a photochemical reactor. After lyophilization, the reaction mixture was purified by RP-HPLC obtaining pure compound **4** as fluffy solid (9 mg, 26%). $^1\text{H-NMR}$ (500 MHz, D_2O): δ 4.72 (overlap with HOD signal); 4.26 (m, 2H); 4.14 (t, 1H, $J = 6.8$ Hz); 4.09 (d, 2H, $J = 7.1$ Hz); 3.98-3.80 (m, 20H); 3.46 (m, 1H); 3.33 (t, 1H, $J = 9.8$ Hz); 3.03 (dd, 1H, $J = 6.0, 14.5$ Hz); 2.93 (dd, 1H, $J = 7.4, 14.5$ Hz); 2.60 (m, 2H); 2.01 (m, 3H); 1.81 (m, 2H); 1.52 (m, 9H); 1.08 (d, 3H, $J = 6.4$ Hz); 0.88-0.70 (m, 36H). MS-MALDI (m/z calcd. for $\text{C}_{65}\text{H}_{114}\text{N}_{17}\text{O}_{23}\text{S}$ $[\text{M}+\text{H}]^+$ 1532.799) (m/z found $[\text{M}+\text{H}]^+$ 1532.83, $[\text{M}+\text{Na}]^+$ 1554.81, $[\text{M}+\text{K}]^+$ 1570.79) analysis.

Allyl 2,3,4,5-tetra-O-acetyl- α -D-galactopyranoside (2b)

Allyl α -D-galactopyranoside **1b** (220 mg, 1 mmol) was treated with acetic anhydride (1.5 mL) and pyridine (0.2 mL), followed by stirring at room temperature overnight. The reaction was slowly poured into DCM (10 mL) and then extracted with 1M HCl (3x 4 mL). The organic layer was washed with saturated NaHCO_3 until the evolution of gasses ceased (2 x 4 mL), and then with water (1 x 4 mL), and brine (1 x 4 mL). The organic phase was dried over MgSO_4 and condensed **2b** as a white solid (360 mg, 94 %). $^1\text{H-NMR}$ spectroscopic analysis of **2b** returned signals in full agreement with literature reference^[30].

Allyl 2,3,4,5-tetra-O-acetyl- α -D-mannopyranoside (2c)

2c was prepared from allyl α -D-mannopyranoside **1c** (110 mg, 0.5 mmol) according to the procedure for **2b** (180 mg, 94 % yield). $^1\text{H-NMR}$ spectroscopic analysis of **2c** returned signals in full agreement with literature reference^[31].

N-Fmoc-L-cysteine-OH (5). Compound **5** was obtained from *N*-Fmoc-L-cysteine(Trt)-OH following reported procedure^[32]. Briefly, *N*-Fmoc-L-cysteine(Trt)-OH (1.0 g, 1.7 mmol) was dissolved in CH_2Cl_2 (50 mL). TFA (1.5 mL, 19.6 mmol) and TIS (0.75 mL) were added to the mixture kept under stirring for 2 hours at room temperature. The solution was basified to pH=9 with Na_2CO_3 , washed with EtOAc and separated. The aqueous solution was acidified with 10M HCl, extracted with EtOAc and concentrated under vacuum. The final product was recovered as an oil and dissolved in $\text{CH}_3\text{CN}:\text{H}_2\text{O}$ (1:4) mixture and lyophilized. The final product was recovered as a white powder (424 mg, 70%). The product was used with no further purification. $^1\text{H-NMR}$ spectroscopic analysis of **5** returned signals in full agreement with literature reference^[32].

Example Procedure for Thiol-ene Coupling to prepare Glyco-Cys Conjugates(6a-c). *N*-Fmoc-L-cysteine **5** (340 mg, 1 mmol), **2a- α** (360 mg, 1 mmol) and DPAP (26 mg, 0.1 equiv) were dissolved in AcOEt (15 mL). The reaction mixture was transferred into quartz tubes and then irradiated under stirring with a Photochemical Multirays Reactor (Helios-Italquartz, Milan, Italy) equipped with ten 15 W lamp whose output was centered at 366 nm for 4 hours. The crude reaction mixture was concentrated under vacuum. The resulting residue was eluted from a column of silica gel (DCM:MeOH, 95/5 v/v) obtaining **6a** as a white solid (200 mg, 30%).

(R)-2-[[[9H-fluoren-9-yl)methoxy]carbonylamino]-3-[[3-(2,3,4-tri-O-acetyl- α -L-rhamnopyranosyl]oxypropylthio]propanoic acid(6a).

$^1\text{H-NMR}$ (500 MHz, $\text{DMSO-}d_6$): δ 7.90 (d, 2H, $J = 7.8$ Hz); 7.70 (d, 2H, $J = 7.6$ Hz); 7.20 (t, 2H, $J = 7.6$ Hz); 7.15 (t, 2H, $J = 7.8$ Hz); 5.06 (m, 1H); 5.03 (m, 1H); 4.85 (t, 1H, $J = 10.0$ Hz); 4.78 (m, 1H); 4.40-4.20 (m, 4H); 4.08 (td, 1H, $J = 9.1, 4.4$ Hz); 3.79 (dq, 1H, $J = 10.0, 6.4$ Hz); 3.67 (m, 1H); 2.91 (dd, 1H, $J = 13.8, 4.6$ Hz); 2.73 (dd, 1H, $J = 13.8, 9.6$ Hz); 2.57 (dt, 2H, $J = 7.0, 3.1$ Hz); 2.07 (s, 3H); 1.99 (s, 3H); 1.90 (s, 3H); 1.79 (m, 2H); 1.08 (d, 3H, $J = 6.4$ Hz). $^{13}\text{C}\{^1\text{H}\}\text{NMR}$ (125 MHz, $\text{DMSO-}d_6$): δ 172.89; 170.22; 170.20; 170.15; 156.47; 144.25; 141.17; 128.13; 127.54; 125.71; 120.56; 97.01; 70.56; 69.50; 69.16; 66.32; 66.18; 66.1; 54.71; 47.09; 33.26; 29.1; 28.55; 21.04; 20.92; 20.87; 17.64.

(R)-2-[[[9H-fluoren-9-yl)methoxy]carbonylamino]-3-[[3-(2,3,4,6-tetra-O-acetyl- α -D-galactopyranosyl]oxypropylthio]propanoic acid(6b). **6b** was prepared from **2b** (320 mg, 0.95 mmol) and **5** (357 mg, 0.95 mmol) according to the procedure for **6a** and recovered as a white solid (365 mg 53% yield). $^1\text{H-NMR}$ (500 MHz, CDCl_3 , TMS): δ 7.68 (d, 2H, $J = 7.8$ Hz); 7.56 (d, 2H, $J = 7.6$ Hz); 7.32 (t, 2H, $J = 7.2$ Hz); 7.21 (t, 2H, $J = 7.5$ Hz); 5.45 (d, 1H); 5.30 (dd, 1H, $J = 10.3, 2.1$ Hz); 5.07 (dd, 1H, $J = 10.6, 2.1$ Hz); 5.01 (d, 1H, $J = 1.6$ Hz); 4.50-4.00 (m, 7H); 3.60 (m, 1H); 3.20 (m, 1H); 3.03 (t, 1H); 2.94 (t, 1H); 2.60 (m, 2H); 2.10 (s, 3H); 1.94 (s, 9H); 1.80 (m, 2H). $^{13}\text{C}\{^1\text{H}\}\text{NMR}$ (125 MHz, CDCl_3): δ 172.99; 170.39; 170.30; 170.21; 169.97; 156.17; 143.94; 133.15; 129.42; 128.22; 126.25; 118.02; 95.26; 73.41; 68.73; 68.12; 68.07; 67.59; 66.33; 56.80; 47.09; 33.26; 29.10; 28.55; 20.75; 20.65; 20.62; 20.60.

(R)-2-[[[9H-fluoren-9-yl)methoxy]carbonylamino]-3-[[3-(2,3,4,6-tetra-O-acetyl- α -D-mannopyranosyl]oxypropylthio]propanoic acid (6c). **6c** was prepared from **2c** (180 mg, 0.50 mmol) and **5** (170 mg, 0.5 mmol) according to the procedure for **6a** and recovered as a white solid (280 mg 76% yield). $^1\text{H-NMR}$ (500 MHz, CDCl_3 , TMS): δ 7.68 (d, 2H, $J = 7.5$ Hz); 7.55 (d, 2H, $J = 7.3$ Hz); 7.32 (t, 2H, $J = 7.5$ Hz); 7.21 (t, 2H, $J = 7.6$ Hz); 5.25 (m br, 1H); 5.23 (m,br, 1H); 5.19 (t, 1H, $J = 2.4$ Hz); 4.71 (m, 1H); 4.50-4.10 (m, 6H); 4.00 (dd, 1H, $J = 12.5, 2.2$ Hz); 3.78 (m, 1H); 3.50 (m, 1H); 3.03 (dd, 1H, $J = 14.3, 3.3$ Hz); 2.88 (dd, 1H, $J = 14.3, 5.4$ Hz); 2.55 (m, 2H); 2.10 (s, 3H); 2.03 (s, 3H); 1.98 (s, 3H); 1.94 (s, 3H); 1.76 (m, 2H). $^{13}\text{C}\{^1\text{H}\}\text{NMR}$ (125 MHz, CDCl_3): δ 172.85; 170.92; 170.27; 170.27; 169.83; 156.92; 143.82; 143.73; 127.65; 127.03; 125.17; 119.87; 95.42; 69.49; 69.27; 68.34; 67.17; 65.96; 62.96; 55.38; 46.95; 34.29; 29.10; 28.87; 20.81; 20.66; 20.62; 20.61.

Peptide-resin GLGGVGLGGVGLGGVG-OH (7) and peptide AcGLGGVGLGGVGLGGVG-OH (7a): SPPS syntheses were accomplished as described in Supporting Information.

Example procedure for preparation of glycosyl-conjugated peptides 9a,b,c.

a) General procedure for manual coupling of cysteine derivatives

The coupling protocol to the peptide-resin **7** was accomplished by using cysteine derivative **6/PyBOP/HOBt**: $\text{H}_2\text{O}/\text{DIPEA}$ (2:2:2) with respect to peptide-resin in DCM:DMF (1:1, v/v) without preactivation. The reaction was carried out for 24 hours at room temperature under continuous shaking. The completeness of amino acid coupling was monitored through the Kaiser testkit (Fluka Analytical, Switzerland). The resin was finally filtrated and washed (3x15mL DMF, 3x20mL DCM). The *N*-terminal Fmoc protecting group was removed from the decorated peptide by 20% piperidine in DMF for three hours.

b) General Procedure for peptide cleavage from Sieber amide resin:

The dry resin was swelled with DCM (10 mL) for 20 minutes in a sealable sintered glass funnel and then the excess of DCM removed. TFA (1% v/v) in dry DCM was added, the funnel was sealed and shaken for 2 minutes. The solution was filtered into a flask containing pyridine in methanol (10% v/v). The filtration was repeated up to 10 times, the resin was washed with DCM (3 x 30 mL) and MeOH. The filtrates were combined and evaporated under reduced pressure to 5% of the initial volume. Diethyl ether was added to the flask in order to aid the precipitation of the peptide. The precipitate was recovered by centrifugation and dissolved in MilliQ water and finally lyophilized obtaining a white fluffy powder.

8a was prepared according to procedures a) and b) from peptide resin **7** (390 mg, 0.145 mmol) and cysteine derivative **6a** (200 mg, 0.29 mmol). ¹H-NMR analysis evidenced that the coupling efficiency was 67%. Small aliquot (5 mg) of crude mixture was purified by RP-HPLC obtaining of pure **8a** (2 mg). ¹H-NMR: (500 MHz, DMSO-*d*₆): δ 8.76 (t, 1H); 8.32-8.10 (m, 7H); 8.03-7.90 (m, 5H); 7.88-7.80 (m, 3H), 7.17 (s, br, 1H); 7.02 (s, br, 1H); 5.06 (d, 1H); 5.03 (dd, 1H), 4.87 (t, 1H); 4.78 (d, 1H); 4.40-4.05 (m, 6H); 4.05-3.60 (m, 22H); 2.99 (m, 2H); 2.61 (t, 2H); 2.09 (s, 3H); 2.02 (s, 3H); 1.92 (s, 3H); 1.97 (m, 3H) 1.83 (m, 2H); 1.57 (m, 3H); 1.46 (m, 6H), 1.08 (t, 3H); 0.85 (m, 36H). MS-ESI (*m/z* calcd. for C₇₁H₁₂₁N₁₈O₂₅S [M+H]⁺ 1657.339) (*m/z* found [M+H]⁺ 1657.884) analysis

8b was prepared according to procedures a) and b) from peptide resin **7** (180 mg, 0.065 mmol) and cysteine derivative **6b** (95 mg, 0.23 mmol). ¹H-NMR analysis evidenced that the coupling efficiency was 60%. Small aliquot (5 mg) of crude mixture was purified by RP-HPLC obtaining pure **8b** (1.5 mg): ¹H-NMR (500 MHz, DMSO-*d*₆): δ 8.76 (t, 1H); 8.32-8.20 (m, 5H); 8.17 (m, 2H); 8.03-7.90 (m, 5H); 7.88-7.80 (m, 3H), 7.17 (s, br, 1H); 7.02 (s, br, 1H); 5.36 (d, 1H); 5.20 (dd, 1H), 5.07 (d, 1H); 4.96 (dd, 1H); 4.40-3.90 (m, 10H); 3.90-3.65 (m, 20H); 3.64 (m, 2H); 2.96 dd, 1H); 2.80 (dd, 1H); 2.63 (t, 2H); 2.12 (s, 3H); 2.03 (s, 3H); 2.00 (s, 3H); 1.97 (m, 3H) 1.94 (s, 3H); 1.83 (m, 2H); 1.59 (m, 3H); 1.46 (m, 6H), 0.85 (m, 36H). MS-MALDI (*m/z* calcd. for C₇₃H₁₂₃N₁₈O₂₇S [M+H]⁺ 1715.853) (*m/z* found [M+H]⁺ 1715.891, [M+Na]⁺ 1737.855) analysis

8c was prepared according to procedures a) and b) from peptide-resin **7** (510 mg, 0.190 mmol) and cysteine derivative **6c** (280 mg, 0.38 mmol). ¹H-NMR analysis evidenced that the coupling efficiency was 65%. Small aliquot of crude mixture was purified by RP-HPLC obtaining pure **8c** (3 mg). ¹H-NMR: (500 MHz, H₂O/D₂O, 9/1, DSS): δ 8.76 (t, 1H); 8.45-8.35 (m, 6H); 8.20 (d, 1H); 8.15-8.05 (m, 5H); 7.95 (d, 1H), 7.90 (d, 1H), 7.88(d, 1H), 7.29 (s, br, 1H); 6.95 (s, br, 1H); 5.25-5.10 (m, 3H); 4.85 (m, 2H), 4.40-4.20 (m, 3H); 4.16-3.90 (m, 8H); 3.88-3.70 20H); 3.55 (m, 2H); 2.99 (m, 2H); 2.63 (t, 3H); 2.09 (s, 3H); 2.02 (s, 3H); 2.01-1.95 (m, 6H); 1.91 (s, 3H); 1.83 (m, 2H); 1.51 (m, 9H); 0.86-0.72 (m, 36H). MS-MALDI (*m/z* calcd. for C₇₃H₁₂₃N₁₈O₂₇S [M+H]⁺ 1715.853) (*m/z* found [M+H]⁺ 1715.958, [M+Na]⁺ 1737.945; [M+K]⁺ 1753.925) analysis

c) Procedure for deacetylation

Crude glyco-conjugated peptides **8a-c** (25 mg of **8a**; 32 mg of **8b** or 62 mg of **8c**) were dissolved in 3-5 mL of a freshly prepared 0.1 M solution of K₂CO₃ in MeOH. The mixture was allowed to react at room temperature under magnetic stirring for 72 hours. The solution was then concentrated under vacuum and the pH was neutralized using HCl 0.1M. The water was finally removed by freeze-drying. The crude glycoconjugated peptides **9a-c** were purified by RP-HPLC.

9a (12 mg, 0.008 mmol): ¹H-NMR (500 MHz, D₂O): δ 4.66 (overlap with HOD signal); 4.26 (m, 3H); 4.04 (m, 4H); 3.94 (m, 1H) 3.90-3.76 (m, 18H); 3.72-3.53 (m, 2H); 3.47 (m, 1H); 3.33 (m, 1H); 3.01 (m, 1H); 2.92

(m, 1H); 2.60 (t, 2H); 2.01 (m, 3H); 1.79 (m, 2H); 1.52 (m, 9H); 1.18 (d, 3H); 0.90-0.72 (m, 36H). MS-MALDI (*m/z* calcd. for C₆₅H₁₁₅N₁₈O₂₂S [M+H]⁺ 1531.81; *m/z* found [M+H]⁺ 1531.72; [M+Na]⁺ 1553.69; [M+K]⁺ 1569.67) analysis.

9b (21 mg, 0.015 mmol) ¹H-NMR (500 MHz, D₂O): δ 4.86 (overlap with HOD signal); 4.81 (overlap with HOD signal); 4.59 (overlap with HOD signal); 4.25 (m, 3H); 4.03 (m, 3H); 3.94-3.76 (m, 21H); 3.75-3.65 (m, 4H); 3.61 (m, 1H); 3.47 (m, 1H); 2.81 (m, 2H); 2.56 (t, 2H); 1.96 (m, 3H); 1.79 (m, 2H); 1.50 (m, 9H); 0.88-0.70 (m, 36H). MS-MALDI (*m/z* calcd. for C₆₅H₁₁₅N₁₈O₂₃S 1547.81) (*m/z* found [M+H]⁺ 1547.85, [M+Na]⁺ 1569.00 [M+K]⁺ 1585.81) analysis.

9c (15 mg, 0.010 mmol): ¹H-NMR (500 MHz, D₂O): δ 4.25 (m, 3H); 4.12 (m, 1H); 4.03 (m, 4H); 3.94 (m, 3H); 3.90-3.75 (m, 18H); 3.66 (m, 2H); 3.50 (m, 2H); 3.02 (m, 1H); 2.92 (m, 1H); 2.60 (t, 2H); 1.99 (m, 3H); 1.80 (m, 2H); 1.51 (m, 9H); 0.86-0.72 (m, 36H). MS-MALDI (*m/z* calcd. for C₆₅H₁₁₅N₁₈O₂₃S 1547.81) (*m/z* found [M+H]⁺ 1547.93 [M+Na]⁺ 1569.69 [M+K]⁺ 1585.88) analysis.

CD Spectroscopy

Circular dichroism spectra were recorded on a JASCO J-815 Spectropolarimeter (JASCO, Milan, Italy), equipped with HAAKE temperature controller. Samples were dissolved at a concentration of 0.1 mg/mL in H₂O and 2,2,2-Trifluoroethanol (TFE) and loaded into cylindrical quartz cells with 1 mm pathlength. Spectra were acquired in a wavelength range of 190–250 nm at 0, 25, 37 and 60 °C, with a scan speed of 20 nm/min and a band width of 1 nm. CD spectra represented the average of 9 scans. The CD spectra were processed using the JASCO Spectral analysis software®. After background subtraction, a FFT filtering algorithm was applied for smoothing, and data expressed as mean residue molar ellipticity [θ]_{MRW} deg cm² dmol⁻¹ residue⁻¹. CD spectra of peptide **3** were carried out in presence of reducing agent 1 mM tris(2-carboxyethyl)phosphine hydrochloride (TCEP).

Turbidimetry

A time coarse measurement was carried out by UV spectroscopy on a Cary 60 UV spectrophotometer (Agilent) equipped with a Peltier temperature controller. The absorbance is expressed as TAA (Turbidity on Apparent Absorbance) as a function of time. The peptides were solubilized in PBS buffer [Phosphate (50 mM), (pH 7.0)] to yield a final concentration of 1 mM, transferred in one cm quartz cuvette kept under stirring at the constant temperature of 37°C. At the end of the turbidity assay, the obtained suspension was centrifuged and the supernatant was removed from the pellet. The pellet was washed with MilliQ water, centrifuged at 13000 rpm for 10 minutes in a HERMLE Z323K and the supernatant removed. The process was repeated twice in order to remove salts. The pellet was suspended in 1 mL of MilliQ water. The suspension was used for AFM, TEM, SEM microscopies and FT-IR spectroscopy, as described in the respective paragraphs.

FT-IR spectroscopy

The samples for FT-IR spectroscopy were analyzed either as lyophilized powder in the pre-aggregation state or recovered from the pellet after turbidimetry studies in the post-aggregation state. The lyophilized peptides and the pellets were mixed with KBr to a final concentration of approximately 1% (w/w). IR spectra were recorded on a Jasco FT-IR-460 spectrometer. Each spectrum is the result of signal-averaging of 256 scans at a resolution of 2 cm⁻¹. All spectra are absorbance spectra after background subtraction. Smoothing of spectra was carried out with a

step of 11 or 13 data points, using the Savitzky–Golay function^[33]. Second derivatives of the spectra were obtained using a step of 13 datapoints to identify discrete absorption bands that make up the complex amide profiles. Quantitative analysis of the individual component bands of amide I was achieved by using the peak fitting module implemented in the Origins ® Software (Microcalc Inc.). In the curve fitting procedure, the Voigt peak shape has been used for all peaks. The Voigt shape is a combination of the Gaussian and Lorentzian peak shapes and accounts for the broadening present in the FT-IR spectrum.

Atomic force microscopy (AFM)

Ten microliters of the suspension were deposited on Silicon (100) wafer substrate (Aldrich, Saint Louis, Mo, USA). The silicon wafers were cleaned by using a two-solvent method consisting in the immersion of Si wafer in warm acetone bath for a period of 10 min. Then a methanol bath for a period of 5 min immediately followed with MilliQ water rinses. Samples were stored in a Petri dish and air-dried overnight at room temperature. Each sample was observed at room temperature by Atomic Force Microscope (Park System XE-120). Data acquisition was carried out in intermittent contact mode at scan rates between 0.2 and 1 Hz, using rectangular Si cantilevers (TAP300Al-G, Budget Sensors) having the radius of curvature less than 10 nm and with the nominal resonance frequency and force constant of 300 kHz and 40 N m⁻¹, respectively.

Transmission Electron Microscopy (TEM)

Twenty microliters of the suspension were deposited onto carbon coated copper grids. Negative staining was performed by applying few drops of 1% uranyl acetate in MilliQ water used to increase the contrast and the electron density of the samples. After air-drying, grids were observed by transmission electron microscopy (Fei Tecnai G2 20 Twin) operating at 100 kV.

Scanning Electron Microscopy (SEM)

Twenty microliters of the suspension were deposited on Silicon (100) wafer substrate (Aldrich, Saint Louis, Mo, USA). Prior to imaging the sample was freeze-fractured after immersion in liquid nitrogen and then mounted using carbon tape on aluminum SEM stubs and sputtered with a thin gold layer. The sample was observed by a scanning electron microscope (Philips-Fei ESEM XL30-LaB6) operating at 30 kV.

Acknowledgements

This work was supported by the following grants: MIUR (PRIN 2010LSH3K). We thank and acknowledge from University of Basilicata, Dr. Maria Antonietta Crudele for technical assistance, Mr. Alessandro Laurita and Mr. Antonio V. Romano (ex-CIGAS) for TEM and AFM images, respectively.

Keywords: Glycopeptides • Elastin • Atomic Force Microscopy • Circular dichroism • Self-assembly

- [1] J. E. Wagenseil and R. P. Mecham, *Birth Defects Res C Embryo Today* **2007**, *81*, 229-240.
[2] B. Bochicchio, A. Bracalello and A. Pepe, *Chirality* **2016**, *28*, 606-611.
[3] a) B. Bochicchio, A. Pepe, M. Crudele, N. Belloy, S. Baud and M. Dauchez, *Soft Matter* **2015**, *11*, 3385-3395; b) L. Gotte, M. G. Giro, D. Volpin and R. W. Horne, *J Ultrastruct Res* **1974**, *46*, 23-33.

- [4] P. Moscarelli, F. Boraldi, B. Bochicchio, A. Pepe, A. M. Salvi and D. Quaglino, *Matrix Biol* **2014**, *36*, 15-27.
[5] O. Seitz, *Chembiochem* **2000**, *1*, 214-246.
[6] a) J. Huang and A. Heise, *Chem Soc Rev* **2013**, *42*, 7373-7390; b) M. Delbianco, P. Bharate, S. Varela-Aramburu and P. H. Seeberger, *Chem Rev* **2016**, *116*, 1693-1752; c) M. Y. Mistou, I. C. Sutcliffe and N. M. van Sorge, *FEMS Microbiol Rev* **2016**, *40*, 464-479.
[7] a) T. Buskas, S. Ingale and G. J. Boons, *Glycobiology* **2006**, *16*, 113R-136R; b) H. Hojo and Y. Nakahara, *Biopolymers* **2007**, *88*, 308-324.
[8] a) Q. Y. Hu, F. Berti and R. Adamo, *Chem Soc Rev* **2016**, *45*, 1691-1719; b) J. M. Langenhan and J. S. Thorson, *Current Organic Synthesis* **2005**, *2*, 59-81.
[9] a) S. Ramesh, P. Cherkupally, T. Govender, H. G. Kruger, F. Albericio and B. G. de la Torre, *Org Lett* **2015**, *17*, 464-467; b) J. Kalia and R. T. Raines, *Angew Chem Int Ed Engl* **2008**, *47*, 7523-7526.
[10] H. C. Kolb, M. G. Finn and K. B. Sharpless, *Angew Chem Int Ed Engl* **2001**, *40*, 2004-2021.
[11] L. M. Campos, K. L. Killops, R. Sakai, J. M. J. Paulusse, D. Dameron, E. Drockenmuller, B. W. Messmore and C. J. Hawker, *Macromolecules* **2008**, *41*, 7063-7070.
[12] A. Dondoni, A. Massi, P. Nanni and A. Roda, *Chemistry* **2009**, *15*, 11444-11449.
[13] K. Griesbaum, *Angew Chem Int Ed Engl* **1970**, *9*, 273-287.
[14] J. R. Kramer and T. J. Deming, *J Am Chem Soc* **2012**, *134*, 4112-4115.
[15] a) W. Chen, L. Gu, W. Zhang, E. Motari, L. Cai, T. J. Styslinger and P. G. Wang, *ACS Chem Biol* **2011**, *6*, 185-191; b) S. Sarkar, S. A. Lombardo, D. N. Herner, R. S. Talan, K. A. Wall and S. J. Sucheck, *J Am Chem Soc* **2010**, *132*, 17236-17246; c) S. Sarkar, A. C. Salyer, K. A. Wall and S. J. Sucheck, *Bioconjug Chem* **2013**, *24*, 363-375; d) P. Karmakar, K. Lee, S. Sarkar, K. A. Wall and S. J. Sucheck, *Bioconjug Chem* **2016**, *27*, 110-120.
[16] S. Balzaretto, V. Taverniti, S. Guglielmetti, W. Fiore, M. Minuzzo, H. N. Ngo, J. B. Ngere, S. Sadiq, P. N. Humphreys and A. P. Laws, *Appl Environ Microbiol* **2016**.
[17] a) L. G. Griffith and S. Lopina, *Biomaterials* **1998**, *19*, 979-986; b) L. Russo and L. Cipolla, *Chemistry* **2016**, *22*, 13380-13388.
[18] J. Zhang, J. Mao, H. Chen and M. Cai, *Tetrahedron: Asymmetry* **1994**, *5*, 2283-2290.
[19] a) Y. M. Angell, J. Alsina, G. Barany and F. Albericio, *The Journal of Peptide Research* **2002**, *60*, 292-299; b) Y. Han, F. Albericio and G. Barany, *J Org Chem* **1997**, *62*, 4307-4312.
[20] a) A. F. Drake, G. Siligardi and W. A. Gibbons, *Biophys. Chem.* **1988**, *31*, 143-146; b) G. Siligardi and A. F. Drake, *Biopolymers* **1995**, *37*, 281-292; c) B. Bochicchio and A. M. Tamburro, *Chirality* **2002**, *14*, 782-792.
[21] E. A. Bienkiewicz, A. Moon Woody and R. W. Woody, *J Mol Biol* **2000**, *297*, 119-133.
[22] A. Perczel, M. Hollosi, P. Sandor and G. D. Fasman, *Int J Pept Protein Res* **1993**, *41*, 223-236.
[23] a) K. Chockalingam, M. Blenner and S. Banta, *Protein Eng Des Sel* **2007**, *20*, 155-161; b) D. E. Meyer and A. Chilkoti, *Nat Biotechnol* **1999**, *17*, 1112-1115.
[24] a) H. Cui, M. J. Webber and S. I. Stupp, *Biopolymers* **2010**, *94*, 1-18; b) R. Orbach, L. Adler-Abramovich, S. Zigerson, I. Mironi-Harpaz, D. Seliktar and E. Gazit, *Biomacromolecules* **2009**, *10*, 2646-2651; c) C. Tang, R. V. Ulijn and A. Saiani, *Langmuir* **2011**, *27*, 14438-14449.
[25] R. Mammadov, A. B. Tekinay, A. Dana and M. O. Guler, *Micron* **2012**, *43*, 69-84.
[26] L. Russo, A. Gautieri, M. Raspanti, F. Taraballi, F. Nicotra, S. Vesentini and L. Cipolla, *Carbohydr Res* **2014**, *389*, 12-17.
[27] D. A. Grant and N. Kaderbhai, *Biochem J* **1986**, *234*, 131-137.
[28] J. Srivastava, A. Khare and N. K. Khare, *Carbohydr Res* **2008**, *343*, 2822-2825.
[29] B. M. Pinto, D. G. Morissette and D. R. Bundle, *Journal of the Chemical Society, Perkin Transactions 1* **1987**, 9-14.
[30] B. Meng, Z. Zhu and D. C. Baker, *Org Biomol Chem* **2014**, *12*, 5182-5191.

- [31] J. P. Utile and B. Priem, *Carbohydr Res* **2000**, 329, 431-439.
- [32] T. H. Wright, A. E. Brooks, A. J. Didsbury, J. D. MacIntosh, G. M. Williams, P. W. Harris, P. R. Dunbar and M. A. Brimble, *Angew Chem Int Ed Engl* **2013**, 52, 10616-10619.
- [33] A. Savitzky and M. J. E. Golay, *Anal. Chem.* **1964**, 36, 1627-1639.

WILEY-VCH

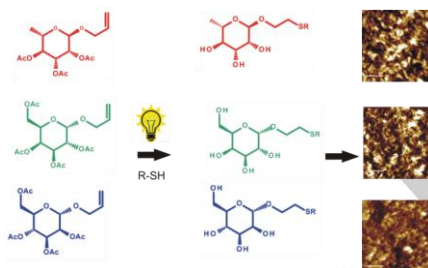
Accepted Manuscript

Entry for the Table of Contents (Please choose one layout)

FULL PAPER

Turn-on light and be sweet.

Glycopeptides synthesis still presents important challenges. The first example of the bioconjugation of a self-assembling elastin-inspired peptide and three carbohydrates has been realized exploiting photo-induced thiol-ene chemistry coupled to Solid Phase Peptide Synthesis. The self-assembly of glycopeptides triggered nanoaggregate formation as shown by AFM and TEM microscopies.



G. Piccirillo, A. Pepe, E. Bedini, and B.Bochicchio* **Page No. – Page No.**

Photoinduced Thiol-ene chemistry applied to the synthesis of self-assembling elastin-inspired glycopeptides